

Viscous decoupling transitions for individually dragged particles in systems with quenched disorder

C. J. Olson Reichhardt and C. Reichhardt

Theoretical Division, Los Alamos National Laboratory, Los Alamos, New Mexico 87545, USA

(Received 11 April 2008; published 10 July 2008)

We show that when an individual particle is dragged through an assembly of other particles in the presence of quenched disorder, a viscous decoupling transition occurs between the dragged particle and the surrounding particles which is controlled by the quenched disorder. A counterintuitive consequence of this transition is that the velocity of the dragged particle can be increased by increasing the strength or density of the quenched disorder. The decoupling transition can also occur when the external drive on the dragged particle is increased and is observable as a clear signature in the velocity-force response.

DOI: [10.1103/PhysRevE.78.011402](https://doi.org/10.1103/PhysRevE.78.011402)

PACS number(s): 82.70.Dd, 74.25.Qt

Recently, several experiments have demonstrated the effectiveness of a local probing technique in which an individual particle is dragged through an assembly of other particles [1–4]. The velocity-force response of the driven particle was measured for a single magnetic colloid pulled through a background of nonmagnetic colloids in Ref. [1], while in other experiments, optical tweezers were used to drive a single colloid through a collection of charge-stabilized colloids [3,4]. Several numerical works have predicted that a rich variety of dynamical regimes can occur in these types of systems depending on whether the probe particle is driven through a glassy media [5–9], a crystal [10], or an assembly of rods [11]. The colloidal dragging experiments are performed on the microscale; however, it is now becoming possible to conduct similar experiments on the meso- and nanoscales. For example, recent experiments have shown that individual vortices in type-II superconductors can be manipulated using a magnetic force microscope tip [12,13]. This technique could be used to study vortex entanglement [14] and the depinning of vortices from extended defects [15]. A simpler initial study would be to measure the drag forces on a single driven vortex in the presence of other vortices and quenched disorder from the sample. Currently, no predictions exist for the response in this regime.

In previous studies of single colloids driven through colloidal assemblies, the driven or probe colloid interacted only with the surrounding colloids. In the superconducting vortex system or in colloidal systems containing random quenched disorder, both the probe particle and the surrounding particles interact with the underlying quenched disorder, which acts as a pinning potential. The addition of pinning might be expected merely to increase the overall drag on the probe particle; however, in this work we show that pinning can induce counterintuitive changes in the probe particle motion since the pinning couples to *both* the probe and the surrounding particles. For example, increasing the strength or density of pinning sites can induce a decoupling transition which sharply *reduces* the effective drag on the probe particle. The same decoupling transition occurs when the driving force on the probe particle is increased and appears as a clear jump in the velocity-force curves. In the strongly damped regime, the probe particle couples strongly to the surrounding particles and induces irreversible plastic deformations. When the pin-

ning strength is increased, the surrounding particles are trapped by pins and cannot respond to the probe particle, so the probe particle decouples from the surrounding particles and the effective damping is reduced. Similarly, when the drive is sufficiently large, the probe particle is unable to induce topological rearrangements in the surrounding particles and a decoupling transition occurs. We specifically examine a system with screened Coulomb particle-particle interactions. Experimentally, this corresponds to a two-dimensional colloidal system with quenched disorder, such as in Ref. [16]. We also study interactions appropriate for vortices in type-II superconductors.

We consider N particles in a two-dimensional sample of size $L \times L$ with periodic boundary conditions in the x and y directions. The overdamped equation of motion for particle i is

$$\eta \frac{d\mathbf{r}_i}{dt} = \mathbf{F}_s^i + \mathbf{F}_p^i + \mathbf{F}_{ext}^i + \mathbf{F}_i^T, \quad (1)$$

where η is the damping constant, which we set to $\eta=1$. The force from particle-particle interactions is $\mathbf{F}_s^i = -F_0 \sum_{i \neq j}^N \nabla V(r_{ij})$, where $F_0 = Z^* / (4\pi\epsilon\epsilon_0)$, Z^* is the unit of charge, ϵ is the dielectric constant of the medium, and the distance between particles located at \mathbf{r}_i and \mathbf{r}_j is $r_{ij} = |\mathbf{r}_i - \mathbf{r}_j|$. We use a Yukawa potential $V(r_{ij}) = \exp(-\kappa r_{ij}) / r_{ij}$, with screening length $1/\kappa = 2$. The quenched disorder is modeled as N_p randomly placed parabolic pinning traps with pinning force $\mathbf{F}_p^i = \sum_k^N f_p(r_{ik}/r_p) \Theta(r_p - r_{ik}) \hat{\mathbf{r}}_{ik}$, where f_p is the pinning strength, $r_p = 0.25$ is the pinning radius, Θ is the Heaviside step function, $r_{ik} = |\mathbf{r}_i - \mathbf{r}_k^p|$, \mathbf{r}_k^p is the location of pin k , and $\hat{\mathbf{r}}_{ik} = (\mathbf{r}_i - \mathbf{r}_k^p) / r_{ik}$. The pinning density is $n_p = N_p / L^2$ and the particle density is $n = N / L^2$. We have examined several different system sizes and present results for $L=48$. For the probe particle, the external driving force $\mathbf{F}_{ext}^i = F_{ext} \hat{\mathbf{x}}$, and for all remaining particles, $\mathbf{F}_{ext}^i = 0$. We construct a velocity-force curve by measuring the time-averaged velocity of the probe particle, $v = \langle \mathbf{v} \cdot \hat{\mathbf{x}} \rangle$, as a function of F_{ext} . The thermal force \mathbf{F}_i^T arises from random Langevin kicks with the properties $\langle \mathbf{F}_i^T \rangle = 0$ and $\langle \mathbf{F}_i^T(t) \mathbf{F}_j^T(t') \rangle = 2\eta k_B T \delta(t-t') \delta_{ij}$. Unless otherwise noted, we set $T=0$. We also consider the case of vortices in type-II superconductors, modeled as in Ref. [17], where $\mathbf{F}_s^i = \sum_{i \neq j}^N f_0 K_1(r_{ij}/\lambda) \hat{\mathbf{r}}_{ij}$. Here K_1 is a modified Bessel

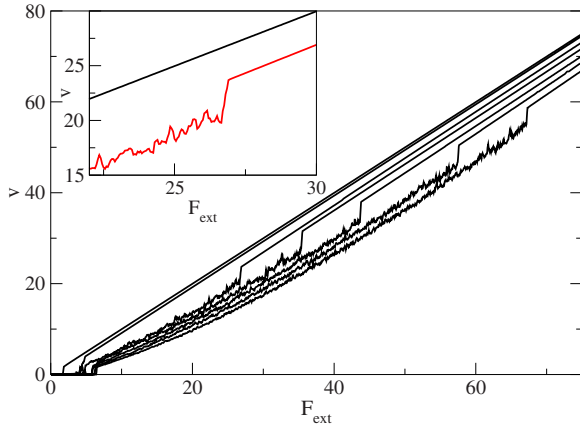


FIG. 1. (Color online) The velocity-force (v - F) curves for a single driven probe particle in a system with $n_p=0.85$ and $f_p=2.0$ at particle densities $n=0, 0.181, 0.292, 0.375, 0.484, 0.53,$ and 0.59 (from top to bottom). Inset: the transition region for $n=0.375$ (bottom) along with the $n=0.181$ curve (top).

function, $f_0 = \phi_0 / (2\pi\mu_0\lambda^3)$, $\phi = h/2e$ is the flux quantum, and λ is the London penetration depth. The probe particle in our system recrosses the same pinned region repeatedly during the course of a measurement; to verify that this does not affect the results, we tested driving forces applied at low angles to the x axis which cause the probe to cross a different portion of the pinned region with each pass through the sample. We find the same results for all driving directions.

We first study a system of Yukawa interacting particles and examine velocity force (v - F) relations for the probe particle in the absence of thermal fluctuations for varying particle densities n . Figure 1 shows the v - F curves for fixed $n_p=0.85$ and $f_p=2.0$ at particle densities ranging from $n=0$ to $n=0.59$. In the limit $n=0$, where the probe particle interacts only with the pinning, there is an initial pinned phase at low drive followed by a transition to a moving state at a critical external drive $F_{ext}^c = 1.7$. In the moving state the particle velocity is proportional to the damping, $v \propto \eta$, representing Ohmic-type behavior. For $n < 0.292$, the v - F curves are similar to the $n=0$ single-particle limit, with only a slight decrease in v in the moving state for increasing n . For $n \geq 0.292$, in addition to the pinned regime at low drive and the Ohmic regime at high drive, we find an intermediate non-Ohmic regime where the velocity undergoes pronounced fluctuations and is reduced below the Ohmic value. Between the non-Ohmic and Ohmic regimes, there is a distinctive jump in the velocity at a drive F_{ext}^t indicating a transition into a moving state with lower damping and reduced velocity fluctuations. The inset of Fig. 1 shows a blowup of the transition region for $n=0.375$; the $n=0.181$ curve is also presented for comparison. As n increases, the velocity of the probe particle in the non-Ohmic regime decreases and the transition drive F_{ext}^t increases.

To illustrate the origin of the different damping in the two moving states, in Fig. 2 we show the trajectories of the probe particle and the surrounding particles in the weakly damped regime at $n=0.3$ and in the strongly damped regime at $n=0.5$. For the weakly damped regime in Fig. 2(a), only small distortions of the surrounding particles occur as the probe

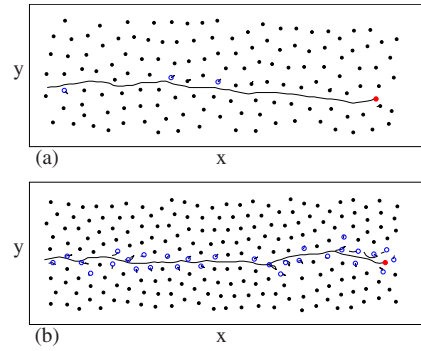


FIG. 2. (Color online) Images of a 38×12 region of a sample with $n_p=0.85$, $f_p=2.0$, and $F_{ext}=8.0$. Large red dot: driven probe particle. Small black dots: unperturbed surrounding particles. Open circles: surrounding particles perturbed by the passage of the probe particle. Lines: particle trajectories. (a) The decoupled moving regime at $n=0.3$ has weak damping. (b) The coupled moving regime at $n=0.5$ has high damping and significant plastic distortions of the surrounding particles.

particle moves through the sample. In contrast, Fig. 2(b) indicates that in the strongly damped regime, the surrounding particles are significantly disturbed by the passage of the probe particle and undergo irreversible plastic distortion events. In order for a plastic rearrangement to occur, a portion of the probe particle energy must be transferred to the surrounding particles, increasing the effective damping on the probe particle. The plastic distortions produce large fluctuations in the probe particle velocity. In the weakly damped regime, the probe particle does not create plastic distortions in the surrounding particles. Thus, the transition we observe between the weakly and strongly damped regimes occurs due to a viscous decoupling transition between the probe particle and the surrounding particles.

The ability of the probe particle to create plastic distortions is affected by the external drive, particle density, pinning strength, and pinning density. In general, a plastic rearrangement occurs when a surrounding particle is both depinned and displaced by a distance $a_0/2$, where $a_0 = n^{-1/2}$ is the average distance between particles. The probe particle spends an average time $\delta t = a_0 / F_{ext}$ interacting with a surrounding particle and exerts a force $F_d = -F_0 \nabla V(a_0/2)$ on the particle. In the absence of pinning, plastic distortions would occur when $-F_0 \nabla V(a_0/2) / F_{ext} > 1/2$, and thus $F_{ext}^t \propto -\nabla V[1/(2\sqrt{n})]$. The v - F curves in Fig. 1 indicate that a transition between the high-damping, plastic motion regime and the low-damping, decoupled regime occurs when the driving force F_{ext} increases. When F_{ext} is large, $F_{ext} \geq F_{ext}^t$, the probe particle passes the surrounding particles so rapidly that it can only induce small displacements due to the short interaction time δt . These displacements are too small to permit plastic rearrangements to occur, and the probe particle decouples from the surrounding particles. For $F_{ext}^c < F_{ext} < F_{ext}^t$, plastic distortions occur and the probe is in the high-damping, coupled motion regime. The lower limit of the coupled motion regime is determined by the fact that the driving force F_{ext} must exceed the critical force F_{ext}^c so that the probe particle itself remains depinned.

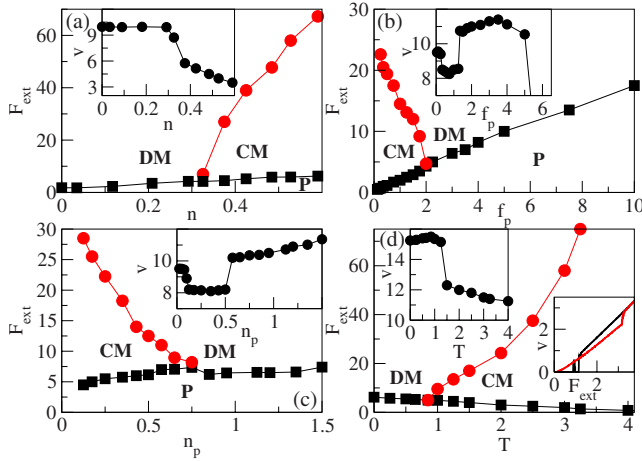


FIG. 3. (Color online) (a) Phase diagram F_{ext} vs n at $f_p=2.0$ and $n_p=0.85$ showing the pinned (P), coupled moving (CM), and decoupled moving (DM) regimes. Squares: depinning threshold F_{ext}^c . Circles: decoupling threshold F_{ext}^t . Inset: v vs n at $F_{ext}=10.0$, showing a drop in v above the transition density of $n=0.3$. (b) Phase diagram for F_{ext} vs f_p at $n_p=0.85$ and $n=0.292$. Inset: v vs f_p at $F_{ext}=12.0$ shows that v can increase with increasing f_p . (c) Phase diagram for F_{ext} vs n_p for $f_p=3.0$ and $n=0.292$. Inset: v vs n_p for $F_{ext}=12.0$. (d) Phase diagram for F_{ext} vs T with $n_p=0.85$, $f_p=3.0$, and $n=0.292$. Left inset: v vs T for $F_{ext}=16.0$. Right inset: v vs F_{ext} for superconducting vortices with $n=0.44$ and $n_p=0.46$. Lower right curve: $f_p=0.25$. Upper right curve: $f_p=1.5$.

Figure 1 shows that the transition drive F_{ext}^t increases with increasing particle density n . This is a result of the increasing strength of the interaction F_d between the probe particle and the surrounding particles with increasing n . At low n , the average distance a_0 between particles is large and F_d is low, so the transition to decoupled motion F_{ext}^t falls at low values of F_{ext} . As n increases, F_d increases due to the decrease in a_0 and the plastic distortions persist up to higher values of F_{ext} , corresponding to a higher value of F_{ext}^t . In Fig. 3(a) we present a phase diagram for F_{ext} versus n taken from a series of v - F curves. The three phases, pinned (P), decoupled moving (DM), and coupled moving (CM), are identified based on the values of F_{ext}^c and F_{ext}^t . The range of driving forces over which coupled motion can occur increases with increasing n . For fixed drive, a velocity drop occurs when n is increased above the coupling-decoupling transition, as illustrated in the inset of Fig. 3(a) for $F_{ext}=10$.

To determine the influence of the pinning on the coupling-decoupling transition, we vary the pinning force f_p in a system with fixed $n=0.292$ and $n_p=0.85$, and plot the resulting phase diagram in Fig. 3(b). The depinning force increases linearly with f_p , $F_{ext}^c \propto f_p$. For very low f_p the system responds as if there were no pinning, a coupled motion regime which was previously explored in Ref. [5]. At low f_p , the probe particle is strongly coupled to the surrounding particles and generates significant plastic distortions. Since the pinning force tends to localize the particles and therefore competes with F_d in determining whether the surrounding particles can undergo plastic motion, we expect plastic distortions to occur in the presence of pinning when $(F_d - f_p) \delta t > a_0/2$, giving $F_{ext}^t \propto F_d - f_p$. This is in agreement with

Fig. 3(b), where F_{ext}^t decreases linearly with f_p . The coupled motion disappears for $f_p > 2.0$ when the probe particle can no longer depin the surrounding particles.

For fixed drive, the probe particle velocity v initially decreases with increasing f_p , as shown in the inset of Fig. 3(b) for $F_{ext}=12.0$. The pinning increases the effective viscosity in the coupled moving regime compared to the $f_p=0$ case by increasing the number of irreversible events that occur. As f_p increases, a surrounding particle that has been depinned and displaced by the probe particle can more easily be repinned at a new pinning site, rather than returning to its previous position in a reversible event. When f_p is further increased, a sharp increase in v occurs at the decoupling transition where the plastic distortions are lost. We note that v in the decoupled regime is *higher* than the value of v at $f_p=0$. These results show that increasing the strength of the pinning can cause a counterintuitive *increase* in the velocity (or decrease in the damping) of the probe particle. At large enough f_p , the probe particle itself becomes pinned.

In Fig. 3(c) we show the phase diagram for F_{ext} versus pinning density n_p for a system with $f_p=3.0$ and $n=0.292$. There is little change in F_{ext}^c with n_p , while F_{ext}^t decreases with n_p until the coupled-motion regime disappears for $n_p > 0.75$. When n_p increases, the average spacing between adjacent pinning sites decreases and a surrounding particle that has been depinned by the probe particle can be trapped by a new pinning site before it has moved far enough to allow a plastic rearrangement to occur. The inset of Fig. 3(c) illustrates the velocity of the probe particle versus n_p at fixed $F_{ext}=12.0$. For very low n_p the behavior is similar to the pin-free case. The effective viscosity increases sharply at $n_p \approx 0.125$ when the system enters the strongly damped, coupled-motion regime. For $n_p > 0.5$, the viscosity drops sharply at the onset of the decoupled motion regime and then monotonically decreases for increasing n_p . Increasing the pinning density can counterintuitively *increase* the velocity of the probe particle v above the value at $n_p=0$.

The phase diagram for F_{ext} versus temperature T is shown in Fig. 3(d) for a system with $f_p=3.0$, $n_p=0.85$, and $n=0.292$. At $T=0$ the probe particle undergoes decoupled motion for $F_{ext} > F_{ext}^c$. As T increases, the effectiveness of the pinning is reduced, F_{ext}^c decreases, and the probe particle recouples to the surrounding particles. This produces a velocity drop with increasing T , as shown in the left inset of Fig. 3(d) for $F_{ext}=16.0$. A transition back to the decoupled moving regime occurs for $F_{ext} > F_{ext}^t$. The overall structure of the phase diagram in Fig. 3(d) is very similar to the dynamical phase diagram for vortices in type-II superconductors moving over random disorder, where a transition from plastic to elastic flow occurs as the driving force on the vortex lattice is increased [18]. Our results indicate that a similar effect can occur even when only a single particle is driven.

We have performed similar simulations for vortices in type-II superconductors. In the right inset of Fig. 3 we plot the v - F curves from a vortex sample with $n_p=0.46$, $n_v=0.44$, and $r_p=0.2$ in the strong-pinning regime with $f_p=1.5$ and in the weak-pinning regime with $f_p=0.25$. The v - F curves have the same trend seen in Figs. 1 and 3(b). The $f_p=0.25$ sample exhibits coupled motion with high damping, while the $f_p=1.5$ sample is in the low-damping, decoupled-

motion regime. A decoupling transition occurs with increasing driving force for the weakly pinned sample. This suggests that our results should be generic to single driven probe particles moving through a background of repulsively interacting particles in the presence of quenched disorder.

In summary, we have shown that when a single probe particle is driven through an assembly of other particles in the presence of quenched disorder, a novel viscous decoupling transition can occur between the probe particle and the surrounding particles which is controlled by the strength and density of the quenched disorder. This transition is from a highly damped regime, where the probe particle depins the surrounding particles and produces irreversible plastic distortions, to a low-damping state, where the probe particle does not couple to the surrounding particles. Increasing the pin-

ning strength or density reduces the coupling between the probe and background particles, producing the counterintuitive result that increasing the strength or density of the quenched disorder *increases* the velocity of the probe particle. The decoupling transition appears as a clear signal in the effective damping on the probe particle and produces a distinct feature in the velocity force curve. In addition to colloids with Yukawa interactions, our results should be general to other systems of interacting particles with quenched disorder, including vortices in type-II superconductors.

This work was carried out under the auspices of the NNSA of the U.S. DOE at LANL under Contract No. DE-AC52-06NA25396.

-
- [1] P. Habdas, D. Schaar, A. C. Levitt, and E. R. Weeks, *Europhys. Lett.* **67**, 477 (2004).
- [2] A. Meyer, A. Marshall, B. G. Bush, and E. M. Furst, *J. Rheol.* **50**, 77 (2006).
- [3] C. Hageman, V. Prasad, and E. R. Weeks, *Bull. Am. Phys. Soc.* **53**, 751 (2008); (unpublished).
- [4] R. P. A. Dullens *et al.* (unpublished).
- [5] M. B. Hastings, C. J. Olson Reichhardt, and C. Reichhardt, *Phys. Rev. Lett.* **90**, 098302 (2003).
- [6] C. Reichhardt and C. J. Olson Reichhardt, *Phys. Rev. Lett.* **96**, 028301 (2006).
- [7] A. S. Khair and J. F. Brady, *J. Rheol.* **49**, 1449 (2005); *J. Fluid Mech.* **557**, 73 (2006).
- [8] S. R. Williams and D. J. Evans, *Phys. Rev. Lett.* **96**, 015701 (2006).
- [9] R. L. Jack, D. Kelsey, J. P. Garrahan, and D. Chandler, e-print arXiv:0803.2002.
- [10] C. Reichhardt and C. J. Olson Reichhardt, *Phys. Rev. Lett.* **92**, 108301 (2004).
- [11] H. H. Wensink and H. Lowen, *Phys. Rev. Lett.* **97**, 038303 (2006).
- [12] E. W. J. Straver *et al.* (unpublished).
- [13] O. M. Auslaender *et al.*, *Bull. Am. Phys. Soc.* **53**, 1010 (2008); (unpublished).
- [14] C. J. Olson Reichhardt and M. B. Hastings, *Phys. Rev. Lett.* **92**, 157002 (2004).
- [15] Y. Kafri, D. R. Nelson, and A. Polkovnikov, *Europhys. Lett.* **73**, 253 (2006); *Phys. Rev. B* **76**, 144501 (2007).
- [16] A. Pertsinidis and X. S. Ling, *Phys. Rev. Lett.* **100**, 028303 (2008).
- [17] C. J. Olson Reichhardt, A. Libál, and C. Reichhardt, *Phys. Rev. B* **73**, 184519 (2006).
- [18] A. E. Koshelev and V. M. Vinokur, *Phys. Rev. Lett.* **73**, 3580 (1994).